

Reconstruction and computation of microscale biovolumes using geographical information systems: potential difficulties

Alexandru I. Petrisor^{a,*}, Adrian Cuc^b, Alan W. Decho^a

^a Department of Environmental Health Sciences, N.J. Arnold School of Public Health, University of South Carolina, Columbia, SC 29208, USA

^b Department of Mechanical Engineering, College of Engineering and Information Technology, University of South Carolina, Columbia, SC 29208, USA

Received 9 October 2003; accepted 24 February 2004

Available online 5 March 2004

Abstract

Biofilms are bacterial colonies enveloped in a matrix of extracellular polymeric secretions. Confocal scanning laser microscopy has been used in conjunction with different image analysis techniques to investigate the structure of biofilms. A major goal is to reconstitute the three-dimensional structure of biofilms, and compute or estimate the biovolumes. Our previous research focused on the utilization of remote sensing techniques and Geographical Information Systems for quantitative analyses of confocal images. The present study investigates potential problems in microbial imaging, and uses two approaches, the program COMSTAT and a Geographical Information Systems-based method, to reconstitute three-dimensional structures and estimate biovolumes. Volumes of thirty fluorescent polymeric microspheres with a known diameter were estimated and used as a ground truth, to statistically compare both methods. In a next step, the two approaches were used to estimate the biovolume of a section through a *Pseudomonas aeruginosa* biofilm. Difficulties were encountered in image acquisition due to the optical properties of the microbeads. Our results indicate that the Geographical Information Systems approach produced results consistent with the existing COMSTAT approach, and close to theoretical values, despite many problems inherent to each phase of this process. Also, the image classification process encountered several limitations. It is suggested that the unique constraints of the microscopic world may generate additional problems, especially related to image classification.

© 2004 Elsevier SAS. All rights reserved.

Keywords: GIS; Biofilm; Bacteria; Image analysis; CSLM; Biovolume

1. Introduction

Biofilms consist of bacterial colonies encapsulated within a matrix of extracellular polymeric secretions (EPS), and form under a range of environmental conditions [24]. The study of biofilms has been facilitated by advances in microscopy, such as the confocal scanning laser microscopy (CSLM) [3,7,13,19] used in conjunction with analytical imaging [9,14], digital analysis [2,12], and semi-automated image processing [10]. Different approaches have been developed based on CSLM in order to assess structure [10] and spatial variability within biofilms [9]. These approaches have allowed the microstructure of biofilms to be observed while in their intact hydrated state. Biofilms are complex environments, where bacterial aggregates are suspended in

polymeric matrices of varying densities and often separated by water canals that form a primitive “circulatory system” and permit enhanced mass transfer [26]. Very often, several species may interact to form specialized “consortia” [16,24].

Bacterial and biofilm images, acquired using analog/nondigital (dark-field microscopy, phase-contrast microscopy, interference microscopy, or fluorescence microscopy) [28], and analytical (CSLM) approaches [11,13], have been processed using various enhancement techniques, such as mathematical filtration, deconvolution, intensity correction, thresholding, cleaning, difference imagery, pseudocolor, contrast stretching [13], and finally image classification [11]. Biofilms have also been analyzed using molecular techniques and, subsequently, digital image analysis [15]. The outcomes of these approaches have included enumeration of bacteria [27], determination of growth, viability, and metabolic condition, assessment of the microstructure of biofilm, microenvironmental analyses [27], quantification of

* Corresponding author.

E-mail address: alexandru_petrisor@yahoo.com (A.I. Petrisor).

biodiversity, and computer control of microscope stage [11]. The concept of “image classification” is used in this paper as a synonym of the “traditional single-stage hard classification” to define the “hard partition of feature space and assignment of each pixel to one of m classes” [8].

In summary, the analysis of two-dimensional images has been well developed [13–15]; however, the application of these techniques to three-dimensional images is problematic.

We propose adding the powerful analytical tools of Geographical Information Systems (GIS) to produce a new image analysis approach. GIS may be defined as a “decision support system involving the integration of spatially referenced data in a problem solving environment” [4]. It can be used to detect changes within biofilms as a result of changing environmental conditions or stressors. Classified images of bacteria are transformed into maps that may be analyzed with GIS and spatial statistical techniques. These analyses may be used to address specific research questions.

Reconstituting the 3-D volume of a biofilm has represented a major focus in studies performed to assess spatial variability within biofilms. An even more important goal has been the computation or at least approximation of the biovolume (volume of the biofilm, in voxels). A special program named COMSTAT has been developed and has become very valuable for computing the area occupied by bacteria in each layer, thickness distribution and mean thickness, fractal dimension, roughness coefficient, distribution of diffusion distances, and surface to volume ratio [6]. These elements have been treated using analysis of variance (ANOVA) to compare the structure of biofilms produced by different species [5]. In addition, textural and areal parameters have been defined to compare various biofilms [12]. Other approaches have used parameters like fractal measurement to extrapolate the two-dimensional results to three dimensions [25]. In other cases, restoration of image volumes has been achieved using inverse volume filtering, correction of geometric distortions, and shading of flat field corrections in conjunction with quantitative analysis techniques [26]. Given that most of these volumetric approaches have been developed recently, Internet-based programs have allowed for the assessment of parameters by simply uploading an image to specific sites (Jan Kreft’s website, <http://www.cf.ac.uk/biosi/staff/kreft/>). For example, websites have been developed (e.g., J. Xavier, Universidade Nova de Lisboa, Portugal) where researchers could submit biofilm images into a database and analyze all images in the database using preset algorithms online (Joao Xavier’s website, http://www.itqb.unl.pt:1111/~jxavier/cur_eng.htm). Finally, many programs such as Image-J, Confocal Assistant or other packages are typically associated with scanning laser confocal microscopes and provide either a method of reconstituting the three-dimensional structures, or a method of estimating the actual volume (Olympus website, <http://www.olympusamerica.com/>).

Our approach does not differ in terms of output, but in terms of methodology [22]. Previous approaches have uti-

lized digital images of biofilms from CSLM in conjunction with fluorescent lectin probes [1,11,12,17,19,20] to develop a tool that will ideally determine or conservatively estimate the volume occupied by bacteria in a certain region of space [21]. Our method illustrates how geographical tools used currently for other purposes (e.g., the 3-D analyst is regularly used to display geomorphologic features) may be used to assess the structure and spatial variability within bacterial biofilms in conjunction with image-processing and remote-sensing techniques, based on images obtained using CSLM, without focusing on the computation of structural parameters. The method is similar in concept to a small-scale application used to calculate the silt volume in Powers Lake, North Dakota [23]. If the average volume(s) of a bacterium is known, then an estimation of the number of bacteria can be performed easily. Applications may include the study of biofilm formation and growth, bacterial colonization, determination of enzymatic activities [22], and quantification of microbially produced mineral precipitates. However, the use of GIS techniques takes a step further than applications of various image-processing techniques, combining it with unique powerful analytical tools. In addition to utilizing this approach for natural systems, as well as calibrating it using fluorescent spheres, we will compare the efficiency of this method with the already existing COMSTAT, based on utilizing fluorescent microspheres as a reference, and unknown volumes of lab-grown colonies [18].

2. Materials and methods

The “scale” of microscopic images is important to ultimately assessing spatial (and temporal) variability in samples; therefore, “calibration” is necessary. In this regard, some authors proposed using fluorescent microspheres of known sizes [18]. The microspheres may be incorporated in gel capsules [18]. The microspheres used in our research are produced by Molecular Probes (T-8883), and called TransFluoSpheres carboxylate-modified microspheres, 1.0 μm (excit./emiss. 488/645 nm). The microspheres have a refractive index of 1.6. Refractive index matching between the lens, lens media and mounting media is very critical. To avoid these interferences, we mounted the beads in oil produced from synthetic hydrocarbons and advanced polymers by Stephens Scientific (M4004), having a refractive index of 1.515. We used a 100 \times oil immersion objective of the Bio-Rad MRC 1024ES confocal scanning laser microscope with the same oil. 30 beads were sampled and five sections through the upper half were obtained for each of them. The thickness of each section was 1 μm , and the distance between sections was 0.2 μm . The output was represented by grayscale image.

Unsupervised (automated) classification of images performed using Erdas Imagine 8.5 was based on generating 2 classes (“beads”, respectively, “biofilm” and background) after a maximum number of 20 iterations per pixel and

a convergence threshold of 0.95 (Erdas Imagine Support, <http://support.erdas.com/>). The output of classification was exported to ArcView GIS 3.2 grid files. For all surfaces, areas were computed in ArcView GIS in pixels.

Volumes were estimated using the formula:

$$V = \sum_{i=1}^5 A_i d = d \sum_{i=1}^5 A_i, \quad (1)$$

where A_i is the area of each section and d is the distance between sections.

Following GIS computations, COMSTAT [5,6] was used to estimate the biovolume in voxels. The original program has been modified to allow for exporting the results in a comma-separated values (CSV) format. Our approach outputs areas in pixels, but COMSTAT expressed areas as percentages of the entire image. The COMSTAT results were converted into cubic μm using the formula:

$$V = \sum_{i=1}^5 A_i \frac{512 \times 512}{100} \frac{1}{10 \times 144.26 \times 144.26}, \quad (2)$$

where 512 is the pixel width/length for each image, and $1/144.26$ is the size of each pixel (computed based on the microscale displayed by the confocal microscope), in μm ; the distance between images was 1 μm .

To test our method on biological samples, a *Pseudomonas aeruginosa* type culture (12121, American Type Culture Collection (ATCC)) was grown on glass microscope slides in 250 ml flasks containing Difco Nutrient Broth, supplemented with dextrose (8 g Difco and 2.5 g dextrose per liter). The medium and bacteria were incubated one week at room temperature prior to analysis. Cells were stained with the nucleic acid stain Syto-9 (Molecular Probes). Slides were visualized using a $100\times$ oil immersion objective of the Bio-Rad MRC 1024ES confocal scanning laser microscope with oil produced from synthetic hydrocarbons and advanced polymers by Stephens Scientific (M4004). Five optical sections, 1 μm thick each, were taken at 0.5 μm from each other.

Images of sections through the biofilm were processed using Erdas Imagine. Briefly, a first step was to enhance images through contrast stretching [8], in order to eliminate the noise and facilitate the separation of bacteria from the background. The method of histogram equalization yielded the best results. In the next step, a 3×3 high pass filter was applied to the enhanced images [8]. Even though structural parameters can be computed for these images using Erdas Imagine, they were not measured in our study. Following processing, images of the sections through the biofilm were classified using unsupervised classification similarly to the images of microspheres and exported to ArcView GIS into a grid format. Following the export to ArcView GIS, all maps were additionally filtered to eliminate noise and produce smooth, continuous surfaces. The five surfaces were overlaid using ArcView GIS, and corresponding areas were computed using the same program.

The following formula was used to convert areas expressed by COMSTAT as percentages of the entire image into pixels:

$$A_P = A_{\%} \frac{1024 \times 1024}{100}, \quad (3)$$

where A_P is the area in pixels, $A_{\%}$ is the area expressed as a percentage of the entire image, and 1024 is the pixel width/length for each image. Volumes were derived using Eq. (1), and the fact that the vertical distance between images was 0.2 μm .

Finally, volumes were computed based on the conversion of voxels into cubic μm using the formula:

$$V_P = \frac{V_{\mu\text{m}^3}}{12.9 \times 12.9}, \quad (4)$$

where V_P is the volume in voxels, $V_{\mu\text{m}^3}$ was the volume in cubic μm , and $1/12.9$ was the size of each pixel in μm (computed again based on the microscale displayed by the confocal microscope).

In addition to the images produced using ArcView GIS, Image J has been used to overlap raw (unclassified) images, producing three-dimensional reconstruction of the volume, displayed in this paper for visualization purposes.

3. Results

The refractive properties of the beads caused several problems, displayed below in Fig. 1, obtained using Image-J.

1. As a result of the loss of axial and lateral resolution, the object becomes less resolute (i.e., becomes “fuzzy”) for deeper images. The problem was less noticeable for beads near the cover slip, but had a more serious impact on the beads deeper into the sample.
2. Due to the refractive index of the beads, two side effects occur. One is to focus the light passing through them, and the other is to attenuate the light intensity [21]. The focusing effect produces a diffraction ring pattern that spreads out from the bead away from the light source.

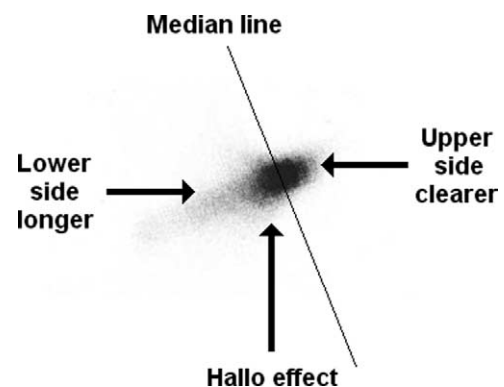


Fig. 1. Distortions caused by the refractive properties of the fluorescent microbeads.

This makes the bead appear to get larger as focusing further. The light attenuation tends to result in a drop off in intensity making the lower half of the bead look dimmer.

To overcome these problems, we used only the upper portion of the bead. Since the vertical distance between the top and bottom sections of each microsphere was 0.5 μm , all computations were adjusted accordingly.

The calibration process was based on the assumption that all beads have a perfect spherical shape and the same diameter of 1 μm . The calibration results are presented in Table 1. The table sums up the calculations of each volume using our approach (column 2) and COMSTAT (column 3). For each set of five images representing halves of beads, the real volume was:

$$V = \frac{1}{2} \frac{4\pi r^3}{3} = \frac{1}{2} \frac{4\pi (d/2)^3}{3} = \frac{\pi d^3}{12} = \frac{3.1415}{12} = 0.2618 \mu\text{m}^3, \quad (5)$$

Table 1

Computation of the volume of upper halves of microspheres using five sections through each sphere (in cubic μm). Results in the second column were obtained using the GIS approach, and the results in the third column were obtained using COMSTAT

Bead	GIS	COMSTAT
1	0.4076	0.4365
2	0.2320	0.2330
3	0.2535	0.2472
4	0.2948	0.3161
5	0.2976	0.3069
6	0.2190	0.2219
7	0.2180	0.2440
8	0.3131	0.3316
9	0.2524	0.2268
10	0.2576	0.2601
11	0.2695	0.2734
12	0.2839	0.2881
13	0.2459	0.2268
14	0.2682	0.2967
15	0.2661	0.2675
16	0.2770	0.2651
17	0.2530	0.2673
18	0.2373	0.2298
19	0.2584	0.2790
20	0.2602	0.2368
21	0.2576	0.2617
22	0.2701	0.2752
23	0.2760	0.3136
24	0.2295	0.2048
25	0.2891	0.3454
26	0.2461	0.2461
27	0.2886	0.3131
28	0.3241	0.3392
29	0.2739	0.2654
30	0.2766	0.2752
Mean:	0.2699	0.2765
Std. dev.:	0.0363	0.0475
95% CI:	(0.2563, 0.2834)	(0.2587, 0.2942)
P-value (testing $H_0: \mu = 0.2618$)	0.232	0.1016

where $d = 2r = 1 \mu\text{m}$ is the diameter of each bead, and r is the radius.

COMSTAT proved once again to be a very useful tool. Beside its already programmed abilities, the flexibility of MathLab programming allowed for optimizations particular to the computers used for this purpose, such as the format of the output etc.; moreover, it allowed for the exploration of optimal threshold value and other parameters that determined the quality of our results.

Fig. 2 displays a reconstruction of the volume of half of the bead using Image-J, overlaying the raw images. The contour of the main diameter was added for a better visualization in PaintShop Pro. Fig. 3 displays the same reconstruction based on our approach.

The results of applying our method to biofilms are displayed below. Fig. 4 is a false three-dimensional image, where the shading intensity (proportional for each layer to its position) gives the three-dimensional appearance of the image. A better image is displayed in Fig. 5 using the 3-D analyst available in ArcView GIS. This tool permits the reconstruction of the volume as well as the rotation of the structure for a better visualization. In comparison, a false three-dimensional image, where the shading intensity (proportional for each layer to its position) gives the three-dimensional appearance of the image obtained using Image-J is displayed in Fig. 6. The results of area computations are presented in Table 2.

Both algorithms use unsupervised classification. However, the classification criterion for COMSTAT is a threshold brightness value. Our method requires specifying the final number of classes (two in our case). The question arising in the first case is, "What is the optimal threshold value?"

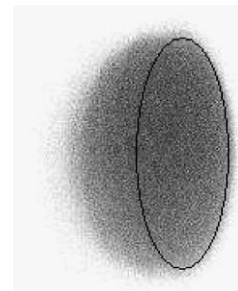


Fig. 2. 3-D reconstitution of the volume of the upper half of a microsphere using Image-J.



Fig. 3. 3-D reconstitution of the volume of the upper half of a microsphere using ArcView GIS.

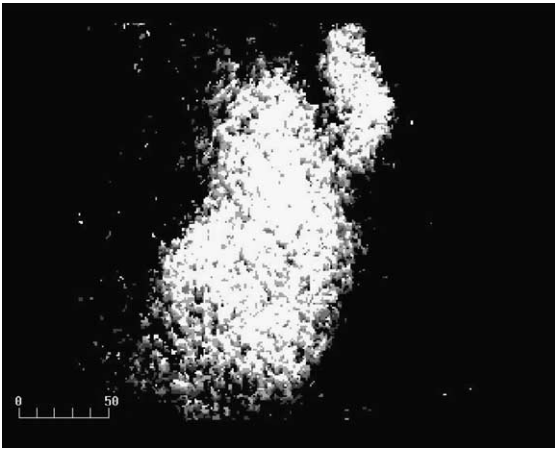


Fig. 4. Image of five overlaid sections through a *P. aeruginosa* biofilm. Shading intensity gives the image a 3-D appearance.

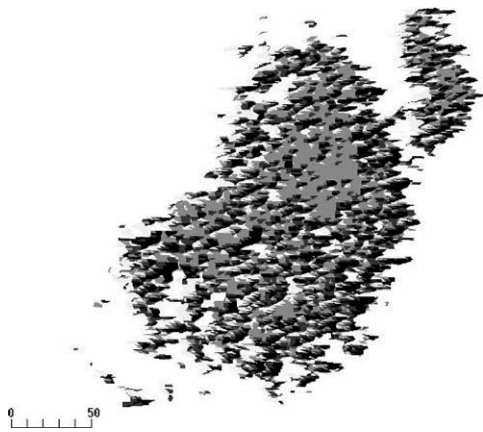


Fig. 5. 3-D reconstitution of the volume based on the five sections through the *P. aeruginosa* biofilm.

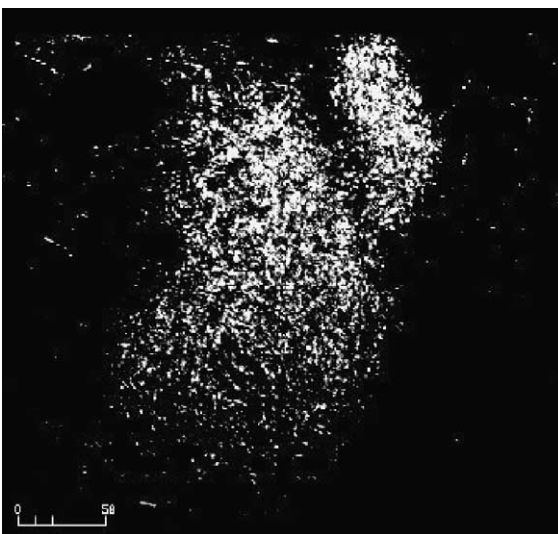
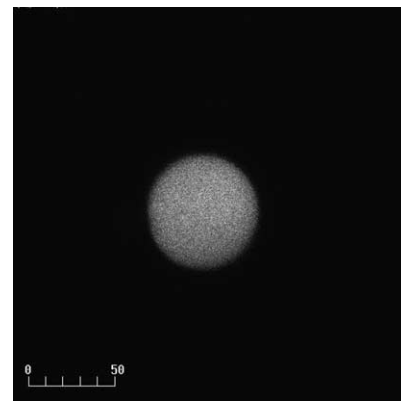


Fig. 6. 3-D reconstruction of the volume based on the five sections through the biofilm obtained using Image-J.

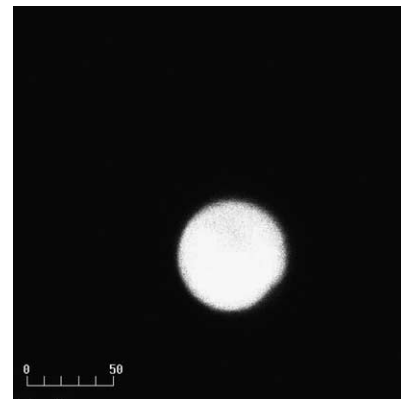
Table 2

Computation of the biovolume using five sections through a *P. aeruginosa* biofilm illustrating the consistency of results using both ArcGIS and COMSTAT approaches

Section	Area computed using ArcGIS (pixels)	Area computed using COMSTAT (pixels)
1	127403.643	74940.678
2	195462.151	102386.106
3	241050.361	120383.865
4	265071.011	132917.494
5	279652.174	133191.172
Volume	656 μm^3	677 μm^3



(A)



(B)

Fig. 7. Differences in brightness intensity between different images. Image A displays a pale color section through a microsphere, whereas Image B shows a very bright section. Differences in brightness may impact image classification.

This is difficult to determine, a priori, even on a gray scale. Without any prior knowledge—that would more likely be a result of accumulated experience, i.e., analyzing as many images as possible, rather than of some scientific reasoning—the “statistical” approach will be to take the half point. That is, based on a gray scale, the middle value between 0 and 255. Pixels with values from 0 to 127 will be classified as “white” and pixels from 128 to 255 as “black”.

In reality, based on their relative position on the mount (3-D position), our objects may appear lighter or darker. To illustrate this, we presented two sections used in our study

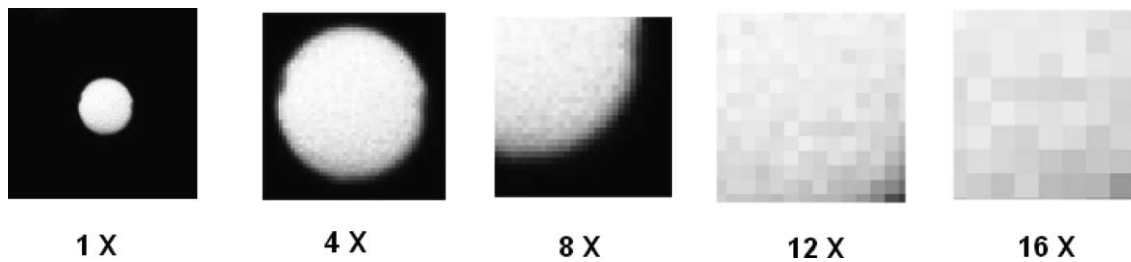


Fig. 8. Sections are not continuous, but collections of pixels of different intensity of light.

(Fig. 7). Image A shows a pale color section, whereas Image B displays a very bright section. Furthermore, there is a large variability in brightness within a certain feature even though it appears continuous, as it represents a collection of pixels of various intensities with a random distribution within a certain range. This may be easily noticed by zooming in an image, as illustrated in Fig. 8.

The problem occurs mostly at the “top” of each image, where there are only few pixels. The top is typically “darker” than the section below. In relationship with the previous paragraph, let us assume we have a “darker” image. If we use the threshold value “128”, all these pixels may be classified as “black” and ignored, and, as a consequence, the area of the section, computed based on the white pixels, is 0. COMSTAT stops here and no volume can be computed. Therefore, we were unable to classify most of the images using the theoretical threshold, 127.

Based on this, we had to decrease the threshold value to 32. That is, the image classification was biased in order to ensure that we “catch” some area within each section. The overall result will be that pixels that will be classified using a threshold value of 128 as “black” will be classified at 32 as “white”. While the initial problem has been overcome, the volumes are computed, and the result is an “artificial” inflation of the volume. This is why COMSTAT estimate was 0.2765, higher than our estimate, 0.2699, and even higher than the theoretical value, 0.2618 (but not high enough to find statistical differences from the theoretical value based on our data, therefore COMSTAT is a very useful tool). It follows that COMSTAT tends to underestimate the volume, since only a biased cut point, favoring pictures classified as “white” (that is, “bead”) will yield an estimate close enough to the theoretical value.

Two examples were used to illustrate these theoretical considerations. The first one is the impact of the halo effect on image classification (Fig. 9). It can be easily noticed that due to this effect, the area does not appear to vary too much across the sections at a threshold value of 8. This is because of the fact that, even though diffraction causes light “dividing” into a bright central area and a low-intensity ring surrounding it, the threshold value detects both the central area (actual section) and the ring, classifying them as a part of the bead.

The strong dependence of the computation on the threshold value is illustrated in Table 3. For each threshold value,

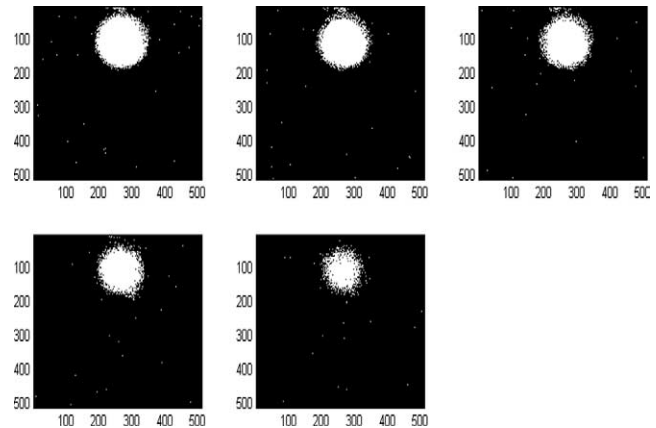


Fig. 9. A threshold value of 8 results into both the diffraction ring and the actual section being classified as part of the bead, determining an enlargement of the area of each section.

images of all five sections were obtained for a representative bead, and volumes were computed in each case. As expected, lower threshold values result in larger estimates of the volume.

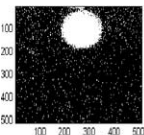
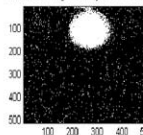
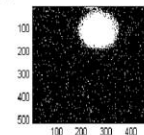
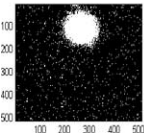
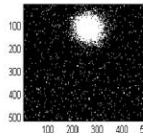
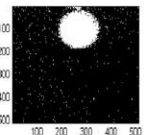
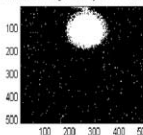
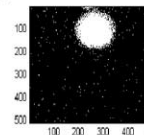
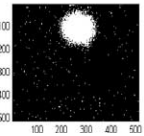
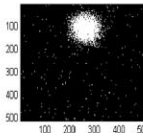
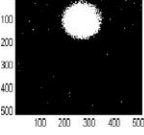
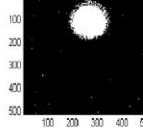
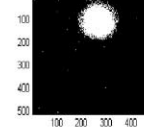
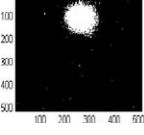
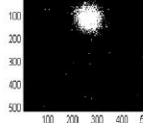
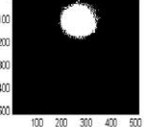
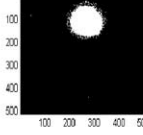
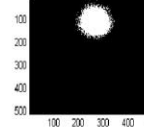
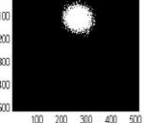
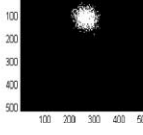
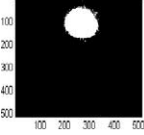
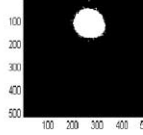
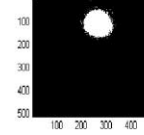
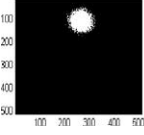
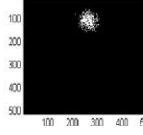
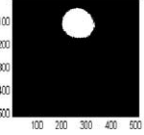
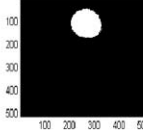
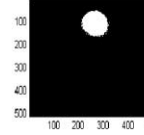
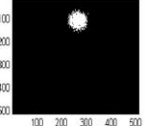
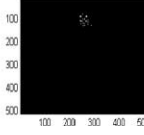
4. Discussion

Image classification techniques rely on the quality of images and are subject to errors introduced at various stages. The suitability of various parameters used currently in image processing in other fields, as well as the choice of various image enhancement techniques should therefore also be judged accordingly. The efficiency of different classification algorithms relies on the quality of the images, visual ability and experience of the researcher, and appropriateness of classification criteria in the second one [8].

In geography, or more precisely when satellite images are analyzed, a “ground truth” is typically obtained [8]. If we analyze the reflected or emitted radiation each component has a certain spectral signature, and, therefore, all features can be identified based on it. However, in microscopic imaging we are dealing with phenomena and structures with a larger variability than typical satellite images [27]. Most of the times, the features contained in each image have very “similar” signatures, i.e., adjacent features are not easily distinguishable.

Table 3

Dependence of the estimate of the volume on the threshold value. Each set of 5 images displays parallel Z-sections

Threshold	Actual image	Vol. (μm^3)	Threshold	Actual image	Vol. (μm^3)
2	    	0.5235	4	    	0.4545
8	    	0.3889	16	    	0.3151
32	    	0.2440	64	    	0.1916

COMSTAT is very flexible and allows experienced researchers to use the appropriate value, allowing for very-fine tuning [5,6]. But when the value is not known, and the optimal value varies from one experiment to another, this advantage is lost.

Our classification is based on always generating two classes at the optimal point as determined by the pixel distribution. The cutoff point differs from one image to another; however the whole procedure is automated and the method is reproducible. Even though it seems more complicated in its application because of using several programs instead of one program, it appears more accurate and also provides a finer control and understanding of the effects of each image manipulation technique. Moreover, even though other programs, such as Image-J (<http://rsb.info.nih.gov/ij/>), permit the visualization of the reconstructed volume, they do not always incorporate the default analytical tools enabling the estimation of volumes. There might be plugins available via the Internet and, in addition, the

software allows Java programmers to develop plugins for specific purposes. Nevertheless, our approach offers the advantage of both visualizing and estimating the volume.

In summary, the cutoff threshold value for COMSTAT is the value from which all images can be properly analyzed and the volume can be properly estimated. This point may be determined through a large enough number of attempts to classify the image. Let us assume that, in our case, this point is 32. Having found this point, we can examine the estimate. It is not statistically different from the theoretical value. Similarly, the estimate our algorithm produced is not statistically different from the theoretical value. Therefore, while different in conception, both methods are valuable tools to resolve the very difficult task of approximating the volume using parallel sections.

Natural biofilms likely exhibit great diversity of bacterial species, and also of sizes and shapes of their bacteria cells [14,24]. The larger relevance of this work is to address a first step in the final goal of the digital image processing

that can be used in conjunction with molecular approaches (e.g., fluorescent in situ hybridization) to potentially identify microbial species, and quantify changes in parameters such as shape and size [27].

Acknowledgements

We acknowledge the helpful insight of Dr. Arne Heydorn (Technical University of Denmark), the laboratory of Dr. Richard Vogt (University of South Carolina), and Mrs. Veronica Karpiak (Molecular Probes). We would also like to thank anonymous reviewers for their helpful comments. This work was supported by National Science Foundation grants EAR-BE 0221796 and MCB-0132528.

References

- [1] R.I. Amann, W. Ludwig, K.H. Schleifer, Phylogenetic identification and in situ detection of individual microbial cells without cultivation, *Microbiol. Rev.* (1995) 143–169.
- [2] D.E. Caldwell, D.R. Korber, J.R. Lawrence, Confocal laser microscopy and digital image analysis in microbial ecology, *Adv. Microb. Ecol.* 12 (1992) 1–67.
- [3] D.E. Caldwell, D.R. Korber, J.R. Lawrence, Imaging of bacteria cells by fluorescence exclusions using scanning confocal laser microscopy, *J. Microbiol. Meth.* 15 (1992) 249–261.
- [4] D.J. Cowen, GIS versus CAD versus DBMS: What are the differences?, *Photogramm. Eng. Rem. Sens.* 54 (1988) 1551–1555.
- [5] A. Heydorn, B.K. Ersboll, M. Hentzer, M.R. Parsek, M. Givskov, S. Molin, Experimental reproducibility in flow-chamber biofilms, *Microbiology* 146 (2000) 2409–2415.
- [6] A. Heydorn, A.T. Nielsen, M. Hentzer, C. Sternberg, M. Givskov, B.K. Ersboll, S. Molin, Quantification of biofilm structures by the novel computer program COMSTAT, *Microbiology* 146 (2000) 2395–2407.
- [7] C.F. Holloway, J.P. Cowen, Development of a scanning confocal microscopic technique to examine the structure and composition of marine snow, *Limnol. Oceanogr.* 42 (1997) 1340–1352.
- [8] J.R. Jensen, *Introductory Digital Image Processing: A Remote Sensing Perspective*, Prentice-Hall, Upper Saddle River, NJ, 1996.
- [9] D.R. Korber, J.R. Lawrence, G.M. Wolfaardt, D.E. Caldwell, Analysis of spatial variability within MOT⁺ and MOT⁻ *Pseudomonas fluorescens* biofilms using representative elements, *Biofouling* 7 (1993) 339–358.
- [10] M. Kuehn, M. Hausner, H.-J. Bungartz, M. Wagner, P.A. Wilderer, S. Wuertz, Automated confocal laser scanning microscopy and semi-automated image processing for analysis of biofilms, *Appl. Environ. Microbiol.* 64 (1998) 4115–4127.
- [11] J.R. Lawrence, D.R. Korber, G.M. Wolfaardt, D.E. Caldwell, Analytical imaging and microscopy techniques, in: C.J. Hurst, G.R. Knudsen, M.J. McInemey, L.D. Stetzenbach, M.V. Walter (Eds.), *Manual of Environmental Microbiology*, ASM Press, Washington, DC, 1997, pp. 29–51.
- [12] J.R. Lawrence, T.R. Neu, G.D.W. Swerhone, Application of multiple parameter imaging for the quantification of algal, bacterial and exopolymer components of microbial biofilms, *J. Microbiol. Meth.* 32 (1998) 253–261.
- [13] J.R. Lawrence, R.T. Neu, Confocal laser scanning microscopy for analysis of microbial biofilms, *Meth. Enzymol.* 310 (1999) 131–144.
- [14] Z. Lewandowski, D. Webb, M. Hamilton, G. Harkin, Quantifying biofilm structure, *Water Sci. Technol.* 39 (1999) 71–76.
- [15] J. Liu, F.B. Dazzo, O. Glagoleva, B. Yu, A.K. Jain, CMEIAS: A computer-aided system for the image analysis of bacterial morphotypes in microbial communities, *Microb. Ecol.* 41 (2001) 173–194.
- [16] R. Losick, D. Kaiser, Why and how bacteria communicate, *Sci. Am.* 276 (1997) 68–73.
- [17] M.N. Mohamed, J.R. Lawrence, R.D. Robarts, Phosphorus limitation of heterotrophic biofilms from the Fraser river, British Columbia, and the effect of pulp mill effluent, *Microb. Ecol.* 36 (1998) 121–130.
- [18] P. Moslemy, S.R. Guiot, R.J. Neufeld, Production of size-controlled gellan gum microbeads encapsulating gasoline-degrading bacteria, *Enzyme Microb. Technol.* 30 (2002) 10–18.
- [19] T.R. Neu, J.R. Lawrence, Development and structure of microbial biofilms in river water studied by confocal laser scanning microscopy, *FEMS Microbiol. Ecol.* 24 (1997) 11–25.
- [20] T.R. Neu, J.R. Lawrence, Lectin-binding analysis in biofilm systems, *Meth. Enzymol.* 310 (1999) 145–152.
- [21] A.I. Petrisor, A.W. Decho, Imaging fluorescent polymeric microspheres using a scanning laser confocal microscope to reconstitute and estimate the volume, in: *Proceedings of the Annual Meeting of the Southeastern Microscopy Society*, vol. 24, 2003, p. 12.
- [22] A.I. Petrisor, A.W. Decho, Using geographical information techniques to quantify the spatial structure of endolithic boring processes within sediment grains of marine stromatolites, *J. Microbiol. Meth.* 56 (2004) 173–180.
- [23] M. Price, Deriving volumes with ArcGIS spatial analyst, *ArcUser* 5 (2002) 52–56.
- [24] P. Stoodley, K. Sauer, D.G. Davies, J.W. Costerton, Biofilms as complex differentiated communities, *Ann. Rev. Microbiol.* 56 (2002) 187–209.
- [25] A. Thill, M. Wagner, J.Y. Bottero, Confocal scanning laser microscopy as a tool for the determination of 3D floc structure, *J. Colloid Interface Sci.* 220 (1999) 465–467.
- [26] M. Wagner, P. Hutzler, R. Amann, Three-dimensional analysis of complex microbial communities by combining confocal laser scanning microscopy and fluorescence in situ hybridization, in: M.H.F. Wilkinson, F. Schut (Eds.), *Digital Image Analysis of Microbes: Imaging, Morphometry, Fluorometry, and Motility Techniques and Applications*, Wiley, New York, 1998, pp. 467–485.
- [27] R.F. Walker, M. Kumagai, Image analysis as a tool for quantitative phycology—A computational approach to cyanobacterial taxa identification, *Limnology* 1 (2000) 107–115.
- [28] F.P. Yu, G. McFeters, Study of biofouling control with fluorescent probes and image analysis, in: L.V. Evans (Ed.), *Biofilms: Recent Advances in Their Study and Control*, Harwood Academic, Reading, UK, 2000, pp. 401–418.